Desalination and Water Treatment
www.deswater.com
doi: 10.1080/19443994.2015.1021848

57 (2016) 8139–8151
April

Taylor & Francis
Taylor & Francis Group

A cast iron filings based model for dynamic investigation of corrosion and its compatibility with the real water distribution network

T. Laskowski[a,*], J. Świetlik[a], U. Raczyk-Stanisławiak[a], P. Piszora[b], M. Sroka[c], A. Olejnik[c], J. Nawrocki[a]

[a]*Faculty of Chemistry, Department of Water Treatment Technology, Adam Mickiewicz University, Umultowska St. 89b, 61-614 Poznań, Poland, Tel. +48 61 829 1582; emails: tomasz.laskowski@amu.edu.pl (T. Laskowski), askas@amu.edu.pl (J. Świetlik), stanisl@amu.edu.pl (U. Raczyk-Stanisławiak), jaceknaw@amu.edu.pl (J. Nawrocki)*
[b]*Faculty of Chemistry, Department of Chemistry of Materials, Adam Mickiewicz University, Umultowska St. 89b, 61-614 Poznań, Poland, Tel. +48 61 829 1262; email: pawel@amu.edu.pl*
[c]*Municipal Water Supply and Sewage Company in Warsaw, Pl. Starynkiewicza 5, 02-015 Warszawa, Poland, Tel. +48 22 445 5852; email: M.Sroka@mpwik.com.pl (M. Sroka), Tel. +48 22 445 5850; email: a.olejnik@mpwik.com.pl (A. Olejnik)*

Received 14 July 2014; Accepted 15 February 2015

ABSTRACT

A new model for the investigation of the impact of corrosion on water quality, based on application of cast iron filings, is proposed. The use of filings ensures a large specific surface area which permits observation of changes in water quality in a relatively small amount of material. Two models differing in idea and construction are presented in this paper. The detailed results from the one model where thin layer water flows over the cast iron filings are shown. The rate of water quality changes during stagnant periods could be controlled by different amounts of filings. The results received in the model experiment are compared with those from a real fragment (100 m) of distribution system. Deterioration of water quality observed in model conditions is similar to that in real distribution network. Increase of iron concentration, turbidity, and decrease of oxygen and nitrate concentration were observed in both systems during stagnation periods. No changes of water quality were observed during flow conditions. Elemental and phase composition of corrosion scales collected from both systems was also comparable.

Keywords: Corrosion; Cast iron; Drinking water; Dynamic model system; Distribution network

1. Introduction

Since the end of the nineteenth century cast iron pipes have become commonly used for water distribution [1–3]. It was soon established that as a result of iron corrosion, the organoleptic properties of water deteriorate. The hardly soluble iron (III) compounds released into water cause an increase in turbidity, change the color, and endow water with a metallic taste [1–7]. Iron (II) contained in the corrosion scale can react with disinfectants, limiting their effectiveness, and increasing the risk of micro-organism regrowth on the scale surface [8–13]. The growth of corrosion scale leads to a reduction in the inside diameter of the pipe and increased roughness of the pipe's interior, which leads to increased costs of water transport. Although recently the use of coated or plastic

*Corresponding author.

pipes is increasing, in many countries, pipes of cast iron and steel make up significant parts of the distribution networks, e.g. in Poland—53% [14], USA —56.6% [15], and Italy—67.2% [16]. The common use of cast iron pipes in the past and the technical and economic problems related to their replacement mean that corrosion will still remain a significant problem for water distributors [17–21].

The effects of corrosion in the water distribution network have stimulated investigations of this phenomenon. The first reports on the corrosion of iron-based materials appeared in the 1920s [4], but only in the middle of the twentieth century were attempts made at explaining the process and eliminating its negative consequences. Because of the complex character of corrosion in the water distribution network, modeling of this process has been a time-consuming and very demanding task. Several approaches to the corrosion process may be found in the literature: changes in water quality are important from the consumers' point of view, while analysis of the corrosion deposits tells us more about the mechanisms of the process. With the help of coupons mounted in such an installation it is possible to estimate the rate of corrosion. The time of experiment is limited by the rate of formation of corrosion deposits, e.g. for the cast iron time varies from 6 to 18 months [22]. The installation of pipelines, tens of meters in length, requires a lot of space, and thus is expensive, shorter fragments of pipes are usually used. Such shorter systems offer a small inner surface area for the observation of corrosion processes, so the investigation of changes in water quality in the flow conditions requires extension of contact time using water recirculation [22,23].

Several papers published recently by Noubactep et al. [24–28] concerning the use of shredded Fe^0 for purification of water inspired us to build similar models based on steel or cast iron filings for investigations into the mechanism of corrosion and the mechanism of water quality deterioration upon corrosion. Thanks to the use of the filings a large surface area on which corrosion could take place was obtained. The BET surface area of an order of a few m^2/g permits simulation of long sections of water distribution pipes with the help of relatively small amounts of cast iron. The first studies with the use of cast iron filings [29] were performed in static conditions. Analysis of the filings' surfaces on which corrosion took place revealed the presence of the same products of corrosion that was identified in the real networks. The proposed experimental model has been designed for investigation of changes in water quality in flowing and stagnant conditions, and for analysis of corrosion scale. The process of corrosion was studied in the laboratory scale and in a pilot station located on a real distribution network, in order to check to what extent the model based on the filings can be used for a simulation of corrosion in a network.

2. Material and methods

2.1. Method

The iron filings were obtained by shredding a fragment of a cast iron pipe from the water distribution system in Warsaw. Prior to fragmentation, the pipe was cleaned of corrosion products. For the experiment, only the fraction of filings with a size of 0.8–1 mm was chosen. The phenomenon of corrosion and changes in water quality was simulated in a flow-through system. To evaluate the mode of water contact with the filings, preliminary studies were performed on two models made of plexiglas, differing in construction and labeled A and B.

The tap water when in contact with the iron filings was subjected to dechlorination over a thin layer of activated carbon, then the suspended matter was removed by a fibrous filter (0.5 μm).

Model A was a container divided into a few parallel sectors. On the bottom of each sector, a thin layer (1–2 mm) of cast iron filings was placed (Fig. 1(a)). Water flowed over the layer. Each sector could be supplied with water of different quality. The rate of water flow was controlled by rotameters (Kyotola, Finland) placed in front of the section. The results obtained from the two sectors in which different amounts of filings were placed are presented in this paper.

A cylinder filled with a bed of cast iron filings and sand mixed at the volume ratio of 2:3 (40 cm^3 of filings, 60 cm^3 of sand) served as model B. Prior to use, the sand was washed out with hydrochloric acid and water, in order to remove any iron contaminants. The sand was used to dilute iron filings preventing their agglomeration. Water was supplied at the bottom of the model and its outflow was at the upper part of the cylinder (Fig. 1(b)). The water flow rate was controlled by a rotameter. Both models are schematically presented in Fig. 1, while their dimensions and the flow rates are given in Table 1. The preliminary experiment was carried out over 36 d. The experiment was divided into periods of water flow, intermittent with 5 periods of 72 h stagnation. About 330 mL of water sample for analysis were collected everyday, and concentrations of iron (III) and total iron, oxygen, turbidity, pH, and conductivity were monitored.

At the next stage, the differences and similarities in the phenomena taking place in the model and in the real water distribution network were analyzed.

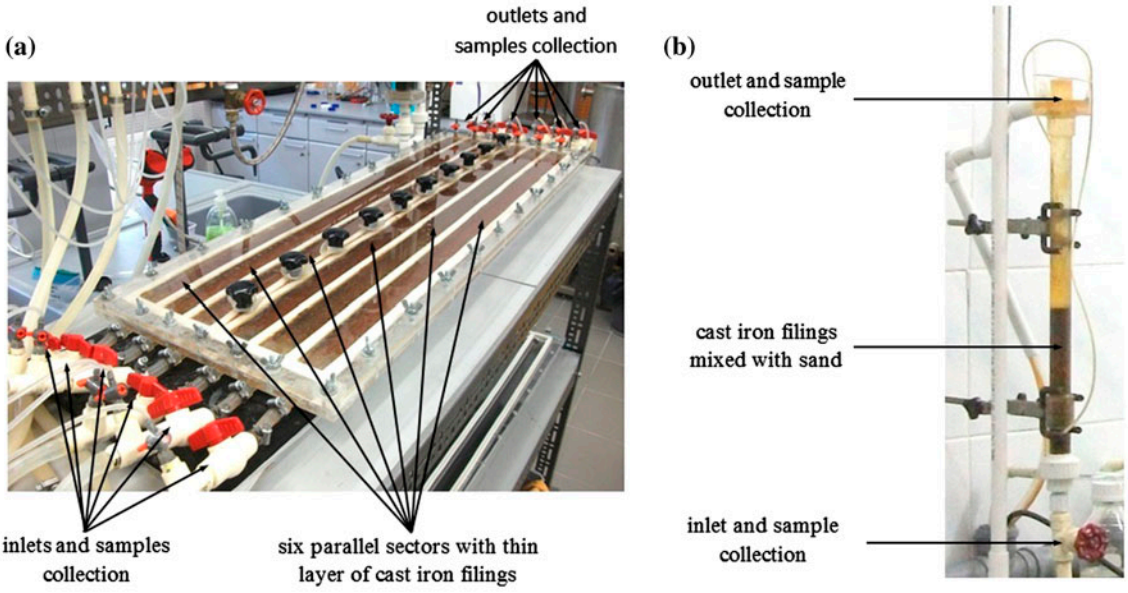

Fig. 1. Presentation of (a): model A and (b): model B.

Table 1
Operation conditions used in model experiments

Dimensions (cm)	Model A (a single sector) 100 × 4 × 2.2 (length × width × height)		Model B 2.5 × 52 (φ × height)
Amount of cast iron filings (g)	110	35	78
Volume flow rate (mL/min)	70		367*/117**
Linear flow rate (cm/min)	79		75*/24**
Contact time in flow conditions (s)	750		16*/ 51**

*First two weeks.
**Further weeks.

For this purpose, model A was selected and a 10-week experiment was performed. Flow conditions and 3, 5, 14, 24, Seventy-two hours stagnant periods were simulated. 72 h stagnation was simulated in each week. Others periods of stagnation were simulated three times between 3–4, 7–8, and 9–10th weeks. The data presented in this paper were obtained in 7–8th week of continuous experiment. Similarly as in the preliminary studies, concentrations of iron (III) and total iron, oxygen, turbidity, pH, and conductivity were monitored. Directly before and after each period of stagnation, the elemental composition of the water was determined by inductively coupled plasma spectroscopy (ICP-OES/MS), its pH was measured along with the concentration of nitrites, nitrates, and ammonium nitrogen. To evaluate impact of the filings amount on the rate of water parameter changes, in two sectors, 110 and 35 g of filings were placed (sectors: A_110, A_35). After completion of the experiment, the phase composition of the corrosion deposit was characterized by X-ray diffraction (XRD) method and their elemental composition was determined by ICP-OES/MS. The scanning electron microscopy (SEM) images of the deposits were taken to analyze their morphology. Analogous measurements were made for the deposits collected from the pipelines from the water distribution network in Warsaw (W1, W2) and Poznań (P1, P2). Sample W1 was the deposit collected at the pilot plant, samples P1 and P2 were collected from the area supplied with the same water as that in the model systems.

The pilot plant was based on a real fragment of approximately 90 year old, 100 m long cast iron pipe of 100 mm in diameter in the existing distribution

system in Warsaw. Before the completion of the plant, a fragment of the pipe was cut off and the corrosion scale was analyzed. The fragment was covered with tubercles (Fig. 2). The cast iron filings used for the experimental model were made of this fragment. The experiment at the pilot station was conducted for 16 weeks under the flow conditions at a flow rate of 0.05 m/s, interspersed with 5, 24, 48, and 72 h periods of stagnation. In conditions of flowing water, the contact time in the pipe was 33 min.

Tap water from Poznan was used to supply the models, while the pilot plant was located in Warsaw. The parameters of the water supplying the model systems were different from those of the water flowing at the pilot plant (see Table 2). The water supplying the models was characterized by a slightly higher pH, higher alkalinity and conductivity and a lower concentration of oxygen than that supplying the pilot plant.

2.2. Analytical methods

2.2.1. Determination of the specific surface area

BET Specific surface area of the iron filings was measured using MICROMETRITICS ASAP 2001 (USA) by adsorption of N_2 at liquid nitrogen temperature. Prior to measurements, the samples were degassed for 4–5 h at 120°C.

Fig. 2. Fragment of the pilot plant pipe with distinct tubercles.

2.2.2. Scanning electron microscopy

The morphology of the filings and corrosion products was evaluated on SEM images taken by a Carl ZEISS EVO 40 SEM scanning electron microscope working at 20 kV. The samples were dehydrated using acetone and covered with gold aerosol using the BALZERS SCD 050 sputterer.

2.2.3. X-ray diffractometry

XRD analysis was performed with the use of a TUR-M62 computer-aided diffractometer equipped with a HZG3 goniometer. Powder diffractograms were recorded with the use of Co Kα radiation and iron filter at an angular range of 6°–90° 2θ. Measurements were made with a step of 0.04° and 5 s pulse time counting at each point of measurement. Prior to the measurements, the samples of corrosion products were pounded to a paste in an agate mortar in a nitrogen atmosphere. The samples, in the form of a dense paste, were placed in a special vessel, covered with a kapton foil and mounted in the optical axis of the goniometer. The phase analysis was performed with the Eva software provided by Bruker in the ICDD PDF2 base. The percentage contents of the crystalline phases identified in the corrosion scales were determined with the help of the PowderCell program.

2.2.4. Fe determination

The concentration of iron in model experiments, was determined by the 2,2-bipyridyl method at $\lambda = 510$ nm, on a Hach DR/2010 spectrophotometer [30].

2.2.5. Metal ions determination

The elements Al, Ca, Fe, Mg, Mn, P, Pb, S, Si, and Zn were identified and quantified in corrosion scales by Varian ICP-OES with Vista-MPX (CCD detector). The concentrations of particular ions were determined after acidification of water with nitric acid (65%, POCH Gliwice, Poland). The corrosion scales were dissolved in hydrochloric acid (35%, POCH Gliwice, Poland). ICP-MS was used for a determination of phosphorous. Details of the methods are provided in [28,31]. Corrosion scales from the model system were prepared for analysis as follows: 2.5 g of iron filings with corrosion scale were suspended in ultrapure water and placed in an ultrasonic bath for 15 min to separate the corrosion products from the cast iron filings. The suspension obtained was collected, dried, weighed, dissolved in HCl and subjected to analysis.

Table 2
Selected parameters water used in model and pilot plant experiments

	Oxygen (mg/L)	Nitrate (mg/L)	pH	Alkalinity (mEq/L)	Conductivity (μS/cm)
Model A and B	6.45	4.37	7.55	3.7	655
Pilot station	8.00	3.8	7.30	2.8	503

2.2.6. Nitrate and nitrite determination

Nitrite and nitrate were determined by ion chromatography (DIONEX ICS-2,500 system) with an ED 50A (Dionex, USA) conductometric detection. An IonPac AS19-HC (4 × 250 mm) analytical column preceded by an IonPac AG19-HG (4 × 50 mm) protective column was used for chromatographic separation of the anions. The details of the method are provided elsewhere [32]. The calibration curve was linear in the range from 5 (detection limit) to 100 mg/L. RSD was smaller than 10% for all anions monitored. Prior to analysis, all samples were filtered through a 0.45 μm filter (Fisherbrand, Fisher Scientific).

2.2.7. Determination of ammonium nitrogen

Ammonium nitrogen was determined by the Nessler colorimetric method [33].

2.2.8. Turbidity

Water turbidity was measured by a Hach 2100P turbidimeter.

2.2.9. Dissolved oxygen

Dissolved oxygen concentration was measured by a Terminal 740 (InoLab) multifunctional device with a StirrOX G (WTW) electrode.

3. Results and discussion

3.1. The dynamic model based on the use of cast iron filings

Both models (A and B) with cast iron filings were used to simulate corrosion of a water distribution system made of cast iron pipes. The models proposed can also be used for investigation of corrosion of other materials used for the construction of water distribution networks or junctions, such as steel, copper, or brass. SEM images of cast iron filings are shown in Fig. 3.

The inner surface of a 1 m long pipe, 100 mm in diameter is 0.314 m^2. The specific surface area of cast iron filings was 1.5 m^2/g. Assuming that the entire surface of the iron filings is in contact with water, then 1 g of the filings corresponds to the inner surface area of 4.75 m of a pipe with a diameter of 100 mm. Therefore, using small amounts of iron filings it is possible to simulate long sections of water distribution pipe, e.g. 110 g of filings would correspond to 522 m long pipe. In our model, the ratio of water volume to the unit of material surface area is an important parameter to be used for comparisons with real systems. The volume of water per unit of surface area in the model A (110 g) was 5.37×10^{-3} dm^3/m^2, while in the real pipe it was 25 dm^3/m^2. So the estimated ratio of water volume to iron surface in the model was 4,650 times smaller than in real conditions. Such a small amount of water in relation to the iron surface should be beneficial when studying changes in water quality. For this reason, the model can approximate the conditions occurring in the neighborhood of corrosion sites. With growing corrosion products, the pores of cast iron filings get blocked, which restricts access to the surface. The filings can also undergo agglomeration. For these reasons, the actual surface area accessible to corrosion processes will decrease with time. Restriction of the access to cast iron surfaces by accumulation of corrosion products and a decrease in the rate of corrosion also take place in real water distribution systems [34,35], however, because of the arrangement of the accessible surface this phenomenon can be more important in the model. A great advantage of the corrosion modeling idea presented is that where the shape and volume of model is chosen, there is still a possibility of regulating the amount of filings. It makes it possible to control the rate and intensity of changes in water parameters arising from corrosion processes. Model A allows simultaneous observation of corrosion processes for six waters with different parameters.

The small volume/surface area ratio facilitates observation of changes caused by corrosion processes, but on the other hand it may be also a disadvantage of the model presented. The lower amount of water in the model also corresponds to a lower amount of oxygen supplied with the water. The small capacity of the model limits the amount of samples of water collected

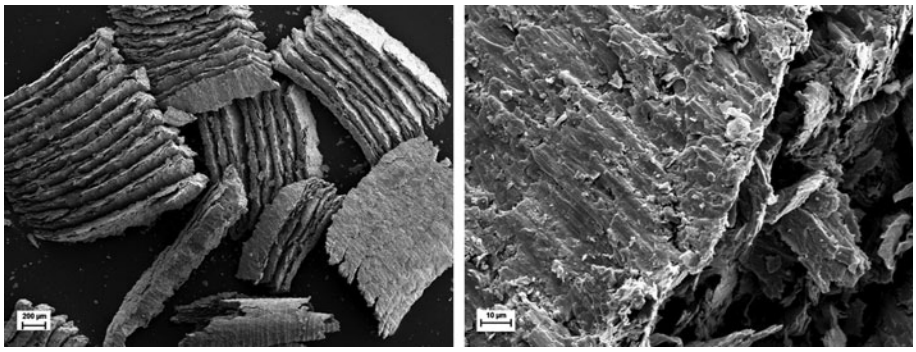

Fig. 3. SEM images of the surface of fresh cast iron filings.

for analysis. The total water volume in one sector of model A is 0.88 L, whereas the water volume in a pipe with the same length (1 m) and 100 mm diameter is 7.85 L. During collection of 330 mL sample, the same volume of "fresh" water, constituting 38% of the total volume, flows into the model sector. This causes dilution of the sample. When sampling the same volume from the 1 m (φ = 100 mm) pipe, only 4% of fresh water is introduced to the system. During sample collection, due to the mixing of fresh and stagnant water, dissolved oxygen concentrations may rise. As a result, some Fe^{2+} in water may be oxidized, which results in the measured Fe^{2+} concentrations being lower than in reality.

It should be realized that there is no model that can simulate conditions identical to those existing in a real distribution network. The main purpose of the presented model is to create the possibility of observing corrosion effects on water quality in a relatively short time. Moreover, we expected to observe more intensive deterioration of water quality compared to a real network.

3.2. Comparison of the two models A and B

In the first stage of the study, the two proposed models, A (110 g of filings) and B, differing in distribution of cast iron filings, were tested. A number of comparative analyses were made to choose the model best simulating conditions in a real distribution network. Changes in water quality were observed in both the flow conditions and after periods of stagnation. In general, the different mode of water contact with iron filings has no effect on the changes in water quality. In the flow conditions, greater changes in the concentrations of iron, oxygen, and in turbidity were observed in model B. Despite the shorter contact time of the water with the cast iron filings, the cast iron/sand bed permitted better contact between the filings and the water than in model A. Moreover, in model B the amount of water per unit area of iron surface was greater, and more oxygen was available than in model A.

However, after periods of stagnation, changes in iron concentrations, turbidity, pH, and conductivity were more visible in model A. The reason for this could be that in model B the stagnant water was mainly above the bed of cast iron filings and only a small volume of water filled the interparticle porosity in the iron–sand bed. The volume of water samples collected from the two models was 330 mL. Since in model B there was a much smaller volume of stagnant water, the analytical samples of water were diluted to a greater degree than those in model A. However, a higher consumption of O_2 was observed in model B. As indicated by these results, such parameters as time and mode of contact, flow rate and the ratio of water to the amount of iron filings can be regulated by the choice of models, depending on the aim of study. Since the type of contact of iron filings with water in the periods of flow and stagnation was more similar in model A to the conditions in the real network and because of the rapid growth in flow resistance with time in model B, model A was selected for further studies.

3.3. Comparison of results obtained in model A and pilot station

3.3.1. Changes in water quality in flow conditions

Corrosion influences water quality in distribution systems. This is probably the most unwanted effect of the process. We measured several parameters of influent and effluent water in both model and pilot station conditions. The parameters were observed for both flow conditions and after different periods of stagnation.

In the flow conditions in the model system as well as in the real network a small increase of total iron concentration and turbidity were observed. Concentrations of dissolved oxygen in both systems were a bit lower at effluent. Because in the model system non-corroded cast iron was used, the greatest increase in total iron concentrations and turbidity was observed on the first day of the experiment and then the Fe concentration systematically decreased over about two weeks before reaching a relatively stable concentration. In general, in flow conditions not much deterioration in water quality was observed in either system (model and real network).

3.3.2. Influence of stagnant periods on water quality

Water stagnation periods in corroded pipes are the main cause of deterioration of water quality. Stagnant water occurs mainly at the terminal sections of distribution networks in the periods of little or no water consumption, such as at night. Long periods of water contact with corrosion scale lead to the disappearance of oxygen in the water and the release of relatively large amounts of Fe(II), which on increased consumption of water can give the red water effect [1,4,36].

3.3.2.1. Iron. In the model, and in the real pipe at the pilot station, the total concentration of iron increased with increasing period of stagnation (Fig. 4). The greatest changes in total iron concentration was observed in effluent from sector A_110. Total iron concentrations increased particularly quickly after 3–14 h stagnation. For periods of stagnation longer than 14 h, total iron concentrations in effluents raised more slowly or did not change (this was observed only in this sector). However, in sector A_35, iron concentrations increased more slowly than in sector A_110. The iron concentration changes for each stagnation period

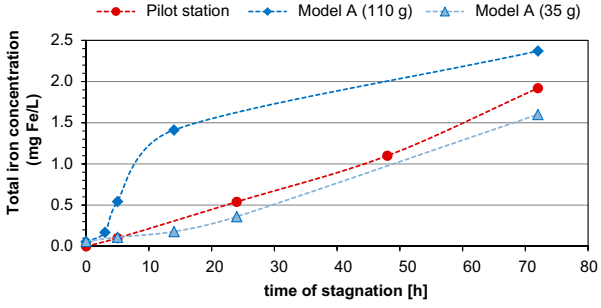

Fig. 4. Changes in the total iron concentration after stagnation conditions, in the model and in the fragment of the real water distribution network.

were comparable with those in the real distribution network. The greatest total iron concentration after 72 h stagnation generally was observed in effluent from sector A_110 (1.59–3.27 mg/L), where 1.04–1.85 mg/L of Fe was found in the effluent of sector A_35, while in the pilot station it was 1.00–1.50 mg/L.

According to Sarin et al. [6] in the period of stagnation, iron is released into the water in the form of Fe^{2+} ions. This suggests that an increase in the concentration of Fe^{2+} can be caused by Kuch's process [37], according to the reaction:

$$Fe_{(metal)} + 2FeOOH_{(scale)} + 2H^{+} \leftrightarrow 3Fe^{2+} + 4OH^{-} \quad (1)$$

or by a release of Fe^{2+} ions present in steady waters [31]. Both in the model and in the fragment of real network studied, the presence of Fe(II) was detected. In the model, the ions appeared as soon as after a 14 h stagnation (in both sectors), while in the fragment of the real network—after 24 h periods of stagnation. The concentrations of Fe(II) in the water from the real network made up 27–69% of the total iron content. In the model, the share of Fe(II) was smaller and reached up to 30% (A_110) or 10% (A_35) of total iron. This difference may follow from the fact that after collecting water samples from the model, a relatively large amount of fresh water was used to flush out the stagnant water. The fresh water contained oxygen, which could oxidize some Fe(II) in stagnation water.

3.3.2.2. Water turbidity. Water turbidity is an important parameter influencing water's esthetic value. In terms of corrosion in a water distribution network, it is closely related to the content of iron (III) as it forms hardly soluble hydroxides suspended in water. Both in the model and in the real network, water turbidity increased with increasing periods of stagnation, as shown in Fig. 5. A greater change in turbidity took place in both sectors of the model system compared to the real distribution network. The highest turbidity value was noted in the A_110 sector. Although the concentration of total iron in sector A_35 and the real distribution network was comparable, higher turbidity was observed in the model. It should be noted that in the pilot station, the pipe concentration of Fe(III) (responsible for water turbidity) was lower. This explains the lower turbidity of the effluent from the pilot station.

3.3.2.3. Concentration of dissolved oxygen. In the model and in the real network fragment studied, the concentration of oxygen decreased with increasing time of stagnation (Fig. 6). The fastest decay of oxygen

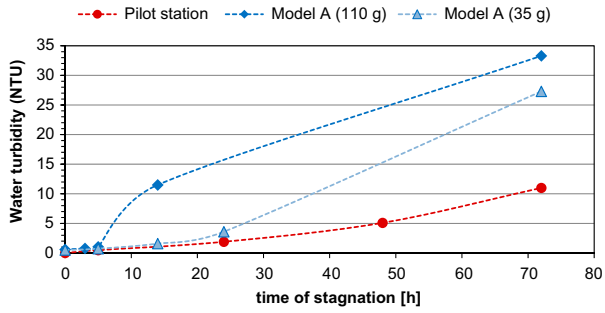

Fig. 5. Changes in water turbidity after stagnation conditions, in the model and in the fragment of the real water distribution network.

concentration was observed in sector A_110. Application of 35 g of filings resulted in a slower rate of oxygen depletion, similar to that in the real distribution network (the surface area of 35 g of filings was 52.2 m^2, while the nominal surface area of internal pipe wall in the pilot station was 31.4 m^2). The different rates of oxygen decay in both sectors were caused by different total surfaces of the corroding material. A larger amount of filings, and thus a larger surface area per water volume resulted in faster oxygen depletion over time. The decrease in oxygen content in particular periods of stagnation is important, as it leads to a release of iron(II) according to Kuch's process. The subsequent supply of oxygen when the flow starts again causes oxidation of Fe^{2+}, which leads to the red water effect [1,37]. Red water phenomena were observed in the model experiments.

3.3.2.4. Nitrates. In the model and in the real network fragment studied, the concentration of nitrates decreased with increasing time of stagnation (Fig. 7). Similarly as for oxygen, the fastest decrease of nitrate concentrations was observed in sector A_110. Total disappearance of nitrates was noted after 14 h of stagnation. The reduction of nitrates to ammonia in the presence of zero valent iron is commonly known [38–40] but the reaction requires acidic conditions. In the presence of green rust, at pH close to neutral, a reduction of nitrates to ammonia is also possible [41–43]. Nitrites are the intermediate products of the reaction of nitrates with FeO [44]. The oxygen-free regions in corrosion deposits make conditions favorable for development of heterotrophic and autotrophic denitrification bacteria [31,45,46]. As a result of denitrification, nitrates are reduced to molecular nitrogen, which does not affect water quality. However, none of the above three mechanisms has been as yet evidenced in corrosion deposits in a real water distribution network. Ammonia was detected in both model sectors as well as in the real distribution network after longer stagnation periods. In some samples of water from the model, small amounts of nitrites appeared. It should be emphasized that, in the model system as well as in the real distribution network, the influent nitrate did not balance with effluent nitrite and ammonia. This indicates the possibility of denitrification during stagnation periods that requires more detailed investigation and explanation.

The results show that in the model based on the cast iron filings, as well as in the real distribution pipe, the same phenomena induced by the corrosion process are observed. Depending on the amount of filings, the intensity of water parameter changes can be regulated. In this work, usage of 110 g of filings caused significantly faster increase of total iron concentrations and turbidity. Also consumption of oxygen and nitrates was fastest in this sector. The rate of water quality changes in sector A_35 was more comparable with that in the real distribution network.

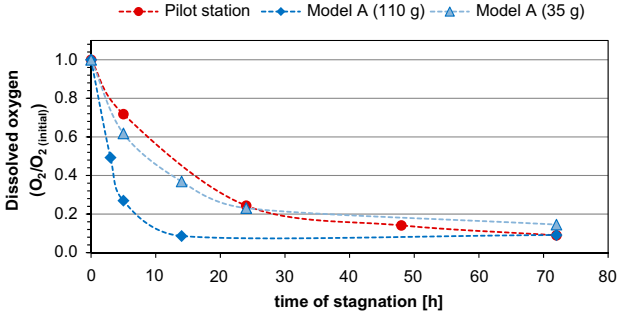

Fig. 6. Decrease in oxygen content in water after stagnant conditions, in the model and in the real water distribution network.

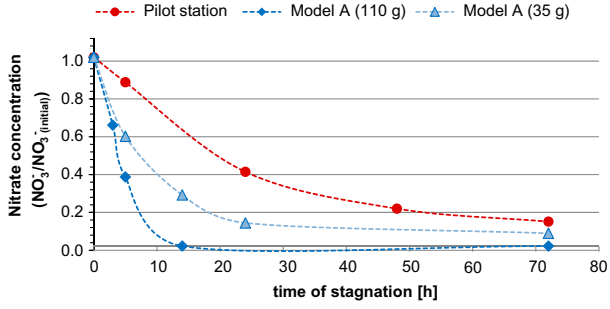

Fig. 7. Decrease in the content of nitrates after periods of stagnation, in the model and in the fragment of the real water distribution network.

3.3.3. Elemental composition of corrosion products

As the composition of corrosion scale depends on the material of the pipe and on the physicochemical parameters of the water, the contents of selected elements in the deposits from model A (110 g of filings) were compared with those in the deposits from the two fragments of cast iron pipes cut out of the water distribution network in Warsaw and from the two sections of pipes from the distribution system in Poznan.

The scales from real networks were dissolved in HCl, the insoluble fraction made from 2.80 to 10.75% of the dry scale mass (Table 3). The insoluble fraction of the corrosion products from the model system made up 13.44%, which is comparable to that obtained for the real network. Iron is the most abundant element in all corrosion scales. The contents of Al, Ca, Mn, P, Pb, and S were similar in both (model and distribution systems) corrosion scales, but the contents of Ca, P, and S were somewhat higher in the scales from the model. The contents of Mg, Si, and Zn in the scale from model A were significantly higher than in all deposits from the real distribution networks studied. However, similar contents of Si and Zn have been found in scales from other water distribution systems [47]. Comparing the differences in the scale compositions, it should be emphasized that the corrosion product from the model was collected after 10 weeks of the experiment—thus at the beginning period of the corrosion process, while the fragments of the real networks were much older (decades). Moreover, it should be realized that the content of elements in the deposits from the real networks sometimes differed by an order of magnitude. The elemental composition of dry corrosion products is shown in Table 3.

The same elements as found in corrosion scales described in this paper have also been identified in the scales studied in [48–53].

3.3.4. The phase composition of corrosion products

XRD was used to assess the composition of the crystalline forms of corrosion scales. The amounts of the scales from the fragments of pipes from the Warsaw and Poznan distribution systems made it possible to analyze individual layers of the scales (E—external and I—internal). Unseparated corrosion scale was analyzed from the model, because of its small amounts. Among the crystalline products of corrosion in the model A system, carbonate green rust and goethite were identified, along with calcite, which is not a corrosion product. The same iron compounds are commonly identified in the scales, as shown by [1,49,53–58]. The presence of calcite in corrosion deposits has been reported in many papers [1,35,45,48,55,58–60]. The scales collected from the Warsaw and Poznan distribution systems contained more crystalline corrosion products, but it should be remembered that this was at the beginning stage of corrosion development in the model. In real systems, goethite is the main component of the external layer of the corrosion scales, but in our model it constituted only 14.8% of the scale. This may be due to the lower availability of oxygen in water, as well as to the early stage of the corrosion process. In the scale from the model, metallic iron comprised 42% of the crystalline phase. For this reason, exact quantitative analysis of the corrosion products would be unreliable. Comparison of the phase composition of corrosion scales was shown in Table 4. The SEM

Table 3
Content of selected elements in dry corrosion scales (% wt.)

Element	Model A (sector A_110)	W1	W2	P1	P2
Al	0.029	0.04	0.0283	0.0017	0.041
Ca	1.904	1.428	0.0747	0.033	0.242
Fe	48.2	33.2	41.3	30.2	41.2
Mg	0.1064	0.0120	0.00203	0.00067	0.0092
Mn	0.1471	0.0500	0.0251	0.0077	0.3000
P	0.1488	0.035	0.089	0.0009	0.120
Pb	0.0017	0.0014	0.0018	0.0009	0.0016
S	0.269	0.0667	0.0492	0.18	0.089
Si	1.164	0.323	0.297	0.0079	0.238
Zn	0.1423	0.0016	0.0130	0.00002	0.0031
Insoluble fraction	13.44	10.75	5.68	2.80	9.06

Notes: W1—deposit from the pilot plant pipe (Warsaw).
W2—deposit from pipeline supplied with the same water as the pilot plant (Warsaw).
P1—deposit from pipeline supplied with the same water as the model system (Poznan).
P2—deposit from pipeline supplied with the same water as the model system (Poznan).

Table 4
Phase composition of corrosion products (% wt.)

		W1		W2		P1		P2	
	Model A (sector A_110)	I	E	I	E	I	E	I	E
GR-(CO_3^{2-})	22.8	33.2	2.8	22.8	8.1	15.7	–	46.6	35.9
GR-(SO_4^{2-})	–	–	4.6	54.3	–	37.8	–	–	3.6
GR-(Cl^-)	–	–	–	6.1	–	46.5	–	22.2	–
Goethite	14.8	48.7	90.4	16.8	79.8	–	98.0	19.3	22.7
Magnetite	–	2.7	2.2	–	10.9	–	–	8.0	25.8
Siderite	–	6.1	–	–	1.2	–	–	4.0	10.7
Lepidocrocite	–	–	–	–	–	–	2.0	–	1.3
Quartz	–	2.0	–	–	–	–	–	–	–
Calcite	20.4	7.0	–	–	–	–	–	–	–
Fe (bcc)	42.0	0.3	–	–	–	–	–	–	–

Notes: W1—deposit from the pilot plant pipe (Warsaw).
W2—deposit from pipeline supplied with the same water as the pilot plant (Warsaw).
P1—deposit from pipeline supplied with the same water as the model system (Poznan).
P2—deposit from pipeline supplied with the same water as the model system (Poznan).
bcc—body-centred cubic (Bravais lattice).
I—internal layer.
E—external layer.

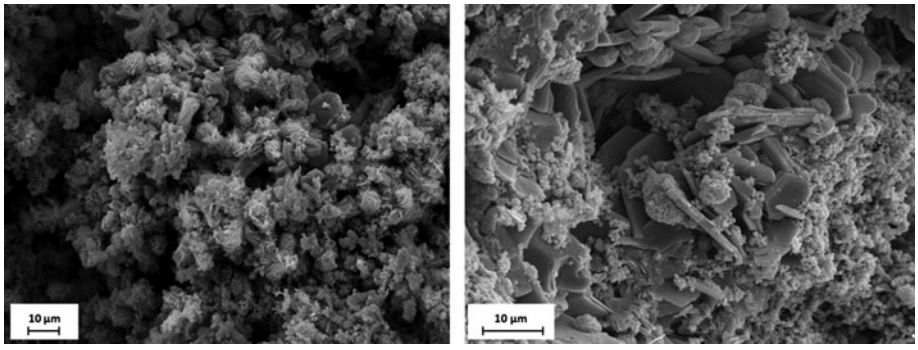

Fig. 8. SEM images of corrosion scales (a) from model A (b) from the real water distribution system.

images of the crystalline products of corrosion present in the deposits from the model and from the real network are presented in Fig. 8 and show similar structures; however, it seems that the crystals observed in Fig. 8(b) are much better developed, perhaps due to the much longer time of the corrosion process.

4. Conclusions

The results show that in the model based on cast iron filings, as well as in the real distribution pipe, the same phenomena induced by the corrosion process are observed. Also, the elemental composition and phase composition of the corrosion scales generated on cast iron filings are similar to that of the corrosion products from the pilot pipe section.

Advantages of model:

(1) The use of filings ensures a large specific surface area, which permits observation of changes in water quality using a relatively small amount of material.
(2) Time and mode of contact, flow rate, and the ratio of water volume to the surface area of iron filings can be easily adjusted by the selection of model.
(3) After selection of model, the rate of water parameter changes during stagnant periods can be also controlled using different amounts of filings.
(4) Model A allows simultaneous observation of the corrosion process for six different waters.

(5) The proposed models are flexible: they can be used with other materials applied for construction of water distribution networks or junctions (such as steel, copper, brass, etc.).
(6) The changes of water quality caused by corrosion may be observed after a relatively short time.

Disadvantages of the model:

(1) Lower amount of water in the model corresponds to a lower amount of oxygen supplied with the water.
(2) Small capacity of the model limits the amounts of water samples collected for analysis.
(3) Sampling after stagnation causes mixing of fresh and stagnant water, and therefore introduces dissolved oxygen. It results with some Fe^{2+} oxidation.
(4) It is difficult to separate the corrosion scale from the filings, and therefore the quantitative analysis of the corrosion scale composition is impossible.

Acknowledgments

The authors wish to acknowledge the financial support from the Polish Ministry of Science and Education within the research grants N N204 339337 and N N523 418737.

References

[1] M.M. Benjamin, H. Sontheimer, P. Leroy, Internal Corrosion of Water Distribution Systems, second ed., in: American Water Works Association Research Foundation (Ed.), Corrosion of Iron and Steel, DVGV Technologiezentrum Wsser, AWWA Research Foundation, Denver, CO, 1996, pp. 29–70.
[2] S.A. Imran, R. Sadiq, Y. Kleiner, Identifying research-needs related to impacts of water quality on the integrity of distribution infrastructure, INFRA 2006, Québec City, November. 20–22, (2006), 1–10.
[3] Health Canada, Guidance on Controlling Corrosion in Drinking Water Distribution Systems. Water, Air and Climate Change Bureau, Healthy Environments and Consumer Safety Branch, Health Canada, Ottawa, Ontario, 2009 (Catalogue No. H128-1/09-595E).
[4] J.R. Baylis, Prevention of corrosion and "red water", J. Am. Water Works Assoc. 15 (1926) 598–633.
[5] M.S. Rahman, G.A. Gagnon, Bench-scale evaluation of drinking water treatment parameters on iron particles and water quality, Water Res. 48 (2014) 137–147.
[6] P. Sarin, V.L. Snoeyink, J. Bebee, K.K. Jim, M.A. Beckett, M.W. Kriven, J.A. Clement, Iron release from corroded iron pipes in drinking water distribution systems: Effect of dissolved oxygen, Water Res. 38 (2004) 1259–1269.
[7] P. Sarin, J.A. Clement, V.L. Snoeyink, W.M. Kriven, Iron release from corroded, unlined cast-iron pipe, J. Am. Water Works Assoc. 95 (2003) 85–96.
[8] A.O. Al-Jasser, Chlorine decay in drinking-water transmission and distribution systems: Pipe service age effect, Water Res. 41 (2007) 387–396.
[9] P.W. Butterfield, A.K. Camper, J.A. Biederman, A.M. Bargmeyer, Minimizing biofilm in the presence of iron oxides and humic substances, Water Res. 36 (2002) 3898–3910.
[10] A.K. Camper, Involvement of humic substances in regrowth, Int. J. Food Microbiol. 92 (2004) 355–364.
[11] L. Kiéné, W. Lu, Y. Lévi, Relative importance of the phenomena responsible for chlorine decay in drinking water distribution system, Water Sci. Technol. 38 (1998) 219–227.
[12] R. Liu, J. Zhu, Z. Yu, D. Joshi, H. Zhang, W. Lin, M. Yang, Molecular analysis of long-term biofilm formation on PVC and cast iron surfaces in drinking water distribution system, J. Environ. Sci. 26 (2014) 865–874.
[13] Z. Zhang, J.E. Stout, V.L. Yu, R. Vidic, Effect of pipe corrosion scales on chlorine dioxide consumption in drinking water distribution systems, Water Res. 42 (2008) 129–136.
[14] M. Kwietniewski, M. Tłoczek, L. Wysocki, Zasady doboru rozwiązań materiałowo-konstrukcyjnych do budowy przewodów wodociągowych (Principles of selecting material and design solutions for the construction of water distribution pipelines), Izba Gospodarcza "Wodociągi Polskie", Bydgoszcz, 2011.
[15] AWWA, Water://Stats 2002 Distribution Survey, AWWA, Denver, CO, 2004.
[16] E. Veschetti, L. Achene, E. Ferretti, L. Lucentini, G. Citti, M. Ottaviani, Migration of trace metals in Italian drinking waters from distribution networks, Toxicol. Environ. Chem. 92 (2010) 521–535.
[17] H. Hotloś, Analiza uszkodzeń i kosztów naprawy przewodów wodociągowych w okresie zimowym [Analysis of failure events and damage repair costs for water-pipe networks in the Winter Season], Och. Srod. 31 (2009) 41–48.
[18] H. Hotloś, Badania zmienności strat wody w wybranych systemach wodociągowych w latach 1990–2008 [Variations in water loss observed in some water distribution systems over the period of 1990–2008], Och. Srod. 32 (2010) 21–25.
[19] A. Kotowski, Analiza hydrauliczna zjawisk wywołujących zmniejszenie przepływności rurociągów [Hydraulic analysis of phenomena reducing pipeline flowability], Och. Srod. 32 (2010) 27–32.
[20] M. Kutyłowska, H. Hotloś, Failure analysis of water supply system in the Polish city of Głogów, Eng. Fail. Anal. 41 (2014) 23–29.
[21] M. Sancy, Y. Gourbeyre, E.M.M. Sutter, B. Tribollet, Mechanism of corrosion of cast iron covered by aged corrosion products: Application of electrochemical impedance spectrometry, Corros. Sci. 52 (2010) 1222–1227.
[22] S.A. Reiber, R.A. Ryder, I. Wagner, Internal Corrosion of Water Distribution Systems, second ed., in: American Water Works Association Research Foundation (Ed.), Corrosion Assessment Technologies, DVGV

Technologiezentrum Wsser, AWWA Research Foundation, Denver, CO, 1996, pp. 445–486.
[23] J.D. Eisnor, G.A. Gagnon, A framework for implementation and design of pilot-scale distribution system, J. Water Supply Res. T 52 (2003) 501–519.
[24] K.B.D. Btatkeu, K. Miyajima, C. Noubactep, S. Caré, Testing the suitability of metallic iron for environmental remediation: Discoloration of methylene blue in column studies, Chem. Eng. J. 215–216 (2013) 959–968.
[25] C. Noubactep, Characterizing the reactivity of metallic iron in Fe $0/U^{VI}/H_2O$ systems by long-term column experiments, Chem. Eng. J. 171 (2011) 393–399.
[26] C. Noubactep, Metallic iron for safe drinking water worldwide, Chem. Eng. J. 165 (2010) 740–749.
[27] C. Noubactep, K.B.D. Btatkeu, J.B. Tchatchueng, Impact of MnO_2 on the efficiency of metallic iron for the removal of dissolved Cr^{VI}, Cu^{II}, Mo^{VI}, Sb^{V}, U^{VI} and Zn^{II}, Chem. Eng. J. 178 (2011) 78–84.
[28] C. Noubactep, S. Caré, Dimensioning metallic iron beds for efficient contaminant removal, Chem. Eng. J. 163 (2010) 454–460.
[29] J. Świetlik, U. Raczyk-Stanisławiak, T. Laskowski, J. Nawrocki, Badania modelowe migracji wybranych pierwiastków z żeliwa i stali do wody na skutek korozji przewodów wodociągowych [Model investigations into the migration of some elements from cast Iron and steel into water due to pipe corrosion], Och. Srod. 33 (2011) 71–76.
[30] F.H. Rainwater, L.L. Thatcher, Methods for Collection and Analysis of Water Samples, U.S. Government Printing Office, Washington, DC, 1968.
[31] J. Nawrocki, U. Raczyk-Stanisławiak, J. Świetlik, A. Olejnik, M.J. Sroka, Corrosion on distribution system: Steady water and its composition, Water Res. 44 (2010) 1863–1872.
[32] J. Świetlik, U. Raczyk-Stanisławiak, J. Nawrocki, The influence of disinfection on aquatic biodegradable organic carbon formation, Water Res. 43 (2009) 463–473.
[33] APHA, Standard Methods for the Examination of Water and Wastewater, eighteenth ed., APHA, Washington, DC, 1992.
[34] L.S. McNeill, M. Edwards, Iron pipe corrosion in distribution systems, J. Am. Water Works Assoc. 93 (2001) 88–100.
[35] P. Sarin, V.L. Snoeyink, D.A. Lytle, W.M. Kriven, Iron corrosion scales: Model for scale growth, iron release and colored water formation, J. Environ. Eng. 130 (2004) 364–373.
[36] J. Nawrocki, J. Świetlik, Analiza zjawiska korozji w sieciach wodociągowych [Analysis of corrosion phenomena in water-pipe networks], Och. Srod. 33 (2011) 27–40.
[37] A. Kuch, Investigations of the reduction and re-oxidation kinetics of iron (III) oxide scales formed in waters, Corros. Sci. 28 (1988) 221–231.
[38] M.J. Alowitz, M.M. Scherer, Kinetics of nitrate, nitrite and Cr(II) reduction by Iron Metal, Environ. Sci. Technol. 36 (2002) 299–306.
[39] S. Choe, H.W. Liljestrand, J. Khim, Nitrate reduction by zero-valent iron under different pH regimes, Appl. Geochem. 19 (2004) 335–342.
[40] Y.H. Huang, T.C. Zhang, Effects of dissolved oxygen on formation of corrosion products and concomitant oxygen and nitrate reduction in zero-valent iron system with or without aqueous Fe^{2+}, Water Res. 39 (2005) 1715–1760.
[41] J. Choi, B. Batchelor, Nitrate reduction by fluoride green rust modified with copper, Chemosphere 70 (2008) 1108–1116.
[42] H.C.B. Hansen, C.B. Koch, H. Nancke-Krogh, O.K. Borggaard, J. Sorensen, Abiotic nitrate reduction to ammonium: Key role of green rust, Environ. Sci. Technol. 30 (1996) 2053–2056.
[43] Y.-L. Tai, B.A. Dempsey, Nitrite reduction with hydrous ferric oxide and Fe(II): Stoichiometry, rate, and mechanism, Water Res. 43 (2009) 546–552.
[44] S. Rakshit, Ch.J. Matocha, G.R. Haszler, Nitrate reduction in the presence of wustite, J. Environ. Qual. 34 (2005) 1286–1292.
[45] X. Li, H. Wang, Y. Zhang, C. Hu, M. Yang, Characterization of the bacterial communities and iron corrosion scales in drinking groundwater distribution systems with chlorine/chloramine, Int. Biodeterior. Biodegrad. 96 (2014) 71–79.
[46] S. Masters, H. Wang, A. Pruden, M.A. Edwards, Redox gradients in distribution systems influence water quality, corrosion, and microbial ecology, Water Res. 68 (2015) 140–149.
[47] Ł. Rudnicka, M. Świderska-Bróż, Skład chemiczny osadów z wrocławskiej sieci wodociągowej [Chemical composition of deposits in Wroclaw' distribution system], Och. Srod. 58 (1995) 63–65.
[48] T.L. Gerke, J.B. Maynard, M.R. Schock, D.L. Lytle, Physiochemical characterization of five iron tubercles from a single drinking water distribution system: Possible new insights on their formation and growth, Corros. Sci. 50 (2008) 2030–2039.
[49] J. Lin, M. Ellaway, R. Adrien, Study of corrosion material accumulated on the inner wall of steel water pipe, Corros. Sci. 43 (2001) 2065–2081.
[50] D.A. Lytle, T. Sorg, L. Wang, A. Chen, The accumulation of radioactive contaminants in drinking water distribution systems, Water Res. 50 (2014) 396–407.
[51] S.C. Morton, Y. Zhang, M.A. Edwards, Implications of nutrient release from iron metal for microbial regrowth in water distribution systems, Water Res. 39 (2005) 2883–2892.
[52] C.Y. Peng, G.V. Korshin, R.L. Valentine, A.S. Hill, M.J. Friedman, S.H. Reiber, Characterization of elemental and structural composition of corrosion scales and deposits formed in drinking water distribution systems, Water Res. 47 (2010) 4570–4580.
[53] O.H. Tuovinnen, K.S. Button, A. Vuorinen, L. Carlson, D.M. Mair, L.A. Yut, Bacterial, chemical and mineralogical characterization of tubercles in distribution pipelines, J. Am. Water Works Assoc. 72 (1980) 626–635.
[54] I.R. McGill, B. McEnaney, D.C. Smith, Crystal structure of green rust formed by corrosion of cast iron, Nature 259 (1976) 200–201.
[55] P. Sarin, V.L. Snoeyink, J. Bebee, W.M. Kriven, J.A. Clement, Physico-chemical characteristics of corrosion scales in old iron pipes, Water Res. 35 (2001) 2961–2969.
[56] J. Świetlik, U. Raczyk-Stanisławiak, P. Piszora, J. Nawrocki, Corrosion in drinking water pipes: The importance of green rusts, Water Res. 46 (2012) 1–10.

[57] F. Yang, B. Shi, Y. Bai, H. Sun, D.A. Lytle, D. Wang, Effect of sulfate on the transformation of corrosion scale composition and bacterial community in cast iron water distribution pipes, Water Res. 59 (2014) 46–57.
[58] Y. Zhu, H. Wang, X. Li, C. Hu, M. Yang, J. Qu, Characterization of biofilm and corrosion of cast iron pipes in drinking water distribution system with UV/Cl_2 disinfection, Water Res. 60 (2014) 174–181.
[59] T.L. Gerke, K.G. Scheckel, R.I. Ray, B.J. Little, Can dynamic bubble templating play a role in corrosion product morphology? Corrosion 68 (2012) 1–7.
[60] F. Yang, B. Shi, J. Gu, D. Wang, M. Yang, Morphological and physicochemical characteristics of iron corrosion scales formed under different water source histories in a drinking water distribution system, Water Res. 46 (2012) 5423–5433.